APPLICATION OF ON-LINE SOLUTION OF 3-DIMENSIONAL MULTIGROUP FINITE-DIFFERENCE NEUTRON DIFFUSION EQUATIONS IN REACTOR POWER CONTROL SYSTEM

by

P.S.W. Chan and M. Mamourian

Atomic Energy of Canada Limited - CANDU Operations Sheridan Park Research Community 2285 Speakman Drive Mississauga, Ontario, L5K 1B2

ABSTRACT

The use of digital computers in on-line control of spatial power distribution, and power manoeuvres has been long established in CANDU reactors. The Power Mapping and Finite Difference (PMFD) method combines the benefits of using diffusion theory with actual measurements of neutron fluxes obtained from self-powered flux detectors to calculate instantaneous channel power and bundle power distributions on-line, for use by the reactor regulating system. The PMFD approach is more accurate than the presently used flux synthesis approach and it is also less sensitive to random and systematic detector errors.

INTRODUCTION

The CANDU reactor regulating system is an integrated system using neutron flux and thermal power measurements, reactivity control devices and a set of digital control computer programs, to perform the following main functions:

- Control total reactor power to a demanded setpoint through bulk power regulation.
- Control reactor power distribution to the nominal power shape in order to avoid violating bundle/channel power limits.
- Move the reactivity control devices at a controlled rate to compensate for various perturbations in reactivity that are encountered during normal and off-normal operation.
- Monitor important plant parameters and reduce reactor power at an appropriate rate if any parameter exceeds its predescribed limit i.e., reactor power setback.

To perform these tasks satisfactorily, the reactor regulating system is required to have the capability to measure deviations in bulk and spatial powers from the specified setpoints, and respond with corrective action to reduce the deviations. While bulk regulation is required to be operational at all power levels, spatial regulation is required to be operational above power levels at which xenon induced power oscillations are possible.

Spatial control in the short term in CANDU 6 is based upon the approximate measurements of the powers of fourteen reactors zones derived from self-powered inconel detectors in each reactor zone, on a two second interval. Consequently, as these measurements are compared with the corresponding reference value of those fourteen signals, an error signal will be generated that will drive the fourteen zone controllers independent of one another, and at a rate proportional to the spatial power error. Accurate long term spatial control is based on the spatial calibration of fast zone power measurements against zone power estimates derived through the processing of accurate vanadium detector signals through the Flux Mapping⁽¹⁾ routine at a frequency of at least two minutes. This program synthesizes the global reactor power distribution using a precalculated set of flux shapes.

In CANDU 6 design, Flux Mapping is also employed in reactor power setback. The flux at selected bundles in the core is estimated using the Flux Mapping program. Reactor power setback is initiated when about 1% of the fuel bundles in the core exceed 110% of operating neutron flux level. Another setback criterion involves the maximum linear heat generation rate during steady and transient operation such as refuelling.

To minimize computing time and memory requirements, some simplistic assumptions have been built into the Flux Mapping program. Amongst them are:

- a. fuel burnup independent flux to power conversion factor, and
- b. smooth harmonic flux shapes calculated from homogenized model, that do not include power ripple due to refuelling.

These assumptions enable the Flux Mapping program to produce a fairly accurate global power shape within a reasonable time using very modest computing resources. However, it also means that Flux Mapping cannot calculate the maximum channel power and the maximum bundle power in a realistic core which has ripples due to refuelling.

The PMFD (Power Mapping Finite Difference) method solves on-line the system of 3-dimensional, 2-energy groups neutron diffusion equations using measured detector fluxes as internal boundary conditions to produce up to date flux and power distributions at any instance. It has the potential of significantly enhancing the performance of the spatial control and the neutronic setback systems.

FLUX/POWER MAPPING OPTIONS FOR SPATIAL REGULATION AND NEUTRONIC REACTOR POWER SETBACK

The design options available for spatial control and setback requirements based on CANDU experience can be summarized as follows:

- Flux Mapping,
- Power Mapping Calibration Routine (PMCR)
- Power Mapping Finite Difference (PMFD)

A brief description about the capabilities of each option is given below.

In the CANDU 6, mapping is carried out by the Flux Mapping program. It collects the readings from the 102 vanadium detectors located throughout the core and performs a least squares fit of this data to the flux modes expected on the basis of the configuration of the reactivity devices. These flux modes are precalculated using time averaged lattice parameters, and as a result the flux maps obtained from Flux Mapping are essentially smoothed distributions which do not recognize localized effects due to burnup variations about the assumed homogeneous values. Flux Mapping cannot calculate accurately the rippled power distributions because of this inherent limitation.

Another Flux Mapping based option used in CANDU 6 is the Power Mapping and Calibration Routine (PMCR), which is executed off-line. PMCR was developed to improve the accuracy in the calculation of channel power using a burnup dependent flux to power correlation. Due to the extensive lattice calculations needed to obtain this correlation, an empirical approach was adopted. The correlation was based essentially on a statistical method made use of the fuelling history of the reactor from a 600 full power day simulation. The flux shapes used in the power and burnup calculations are however, based on the smooth time averaged shapes.

The limitations of Flux Mapping and PMCR led to the development of a fast on-line power mapping technique, which is based on the calculation of instantaneous power distributions. Power Mapping with Finite Difference (PMFD) method uses a finite difference technique to solve the two energy group, 3-D neutron diffusion equations, with the vanadium detector readings used as internal boundary conditions. The solution of the diffusion equation is performed on-line for every fuel bundle. Bundle irradiations are updated via a fuel burnup routine at the end of every power calculation. For reactor control purposes, especially during transients, xenon history can be tracked explicitly.

GENERAL DESCRIPTIONS OF PMFD

In recent years, there has been significant interest in using Slightly Enriched Uranium (SEU) in CANDU reactors. These SEU reactors, which use fuel enrichments up to 1.5 wt % U-235, give significantly better fuel burnup and power uprating potentials than the natural uranium fuelled reactors⁽²⁾.

The higher fissile content and the higher fuel burnup of SEU reactors result in higher power ripples than those in the natural uranium fuelled reactors. Also, concerns of fuel integrity at high burnup require accurate on-line monitoring of individual channel and bundle powers. The present Flux Mapping program cannot meet the requirements of CANDU SEU reactors.

PMFD combines theory and measurements to produce up to date channel and bundle powers in the reactor core at any instance. It is designed to replace the Flux Mapping program in the control system of CANDU SEU reactors. However, it can be easily implemented in existing CANDU stations as an independent on-line power monitoring and fuel management program.

APPLICATIONS

The PMFD program can be used in two modes, i.e., simulation mode and prediction mode. In the simulation mode, PMFD calculates fluxes and powers in the core based on input information such as channels refuelled, reactor power level, control-device positions, and flux detector readings. In this mode PMFD simulates what has already happened in the reactor. The simulated results can be used to compare with available measurements. A good agreement between simulation and measurements assures the reactor operators that the reactor is operating as expected. However, the real benefit of implementing PMFD on-line is due to the ability of PMFD to predict how the reactor will respond to a certain action before that action actually takes place. This prediction is not limited by preconceived situations. It is based on the most current status of the reactor. Furthermore, it is available on demand, i.e., at the very instance when intelligent information is needed. For example, a reactor operator can consult the PMFD program to determine if it is safe to change the reactor power, to refuel a certain channel, or to raise a certain bank of adjuster rods under the current reactor conditions. Programs such as Flux Mapping and PMCR cannot operate in the predictive mode.

FORMALISM

PMFD uses a line iteration technique to solve for the 3–D neutron flux distribution in the core. The neutron flux at every mesh point along a channel is solved using a finite-difference numerical scheme commonly known as "forward elimination and backward substitution", which is well established^(3, 4). Although this numerical scheme is well known, the incorporation of measured flux values as internal boundary conditions is a unique feature.

EXTERNAL BOUNDARY CONDITIONS

Figure 1 shows a single channel with N axial mesh points. The flux distribution along the channel is solved as a boundary value problem. The boundary conditions are usually specified as the distances from the boundaries where the neutron flux extrapolates to zero. The flux gradients at the boundaries, i.e., at n=1 and n=N, can be derived from the extrapolation distances. The conventional finite-difference method uses these external boundary conditions to solve for the flux distribution between the boundaries.

INTERNAL BOUNDARY CONDITIONS

Figure 2 shows a channel with N axial mesh points where a measured flux value Φ_d is available at mesh d. The flux solution is split into two lines. The first line extends from n=1 to n=d-1 and the second line from n=d+1 to n=N. The measured flux, Φ_d , determines the flux gradients at n=d-1 and at n=d+1. Therefore Φ_d can be considered as an internal boundary condition. In general, a channel with m measured flux values will be split into (m+1) lines for flux solution purposes. The resulting flux distribution satisfies the following constraints:

- i. the zero flux boundary conditions at either end of the channel,
- ii. the distribution of lattice properties within the channel, and
- iii. the measured flux values.

TRANSFORMATION OF MEASURED DETECTOR FLUXES INTO PMFD MESH FLUXES

Flux detectors are placed interstitially between fuel channels. The physical locations of the detectors do not coincide with the coordinates of the mesh points in the PMFD model. In order to use the measured detector readings as internal boundary values in the PMFD calculations, it is first necessary to transform the detector readings into the appropriate PMFD "measured fluxes".

The program INTREP is routinely used to calculate theoretical detector fluxes at Flux Mapping and ROP (Regional Overpower Protection) detector locations by interpolation of mesh fluxes calculated by an off-line fuel management program. The inverse of this procedure is used to transform measured detector fluxes into PMFD measured mesh fluxes. The transformation procedure is given below:

- Run the PMFD code with the most recent fuel burnup distribution and reactivity device positions. Record the Flux Mapping detector readings, but calculate the core flux distribution without using the detector readings.
- ii. Use INTREP to calculate the theoretical fluxes at the Flux Mapping detector locations based on the theoretical PMFD core fluxes.
- iii. Calculate $T_{\rm dj}$, the flux ratio between the detector flux and the PMFD mesh fluxes for the 8 meshes which are closest to the detector, using the formula

$$T_{dj} = \frac{\Phi_j}{\Phi_d}$$

where

 Φ_d = flux at detector d calculated by INTREP using PMFD mesh fluxes

 Φ_i = PMFD mesh flux of the j-th mesh closest to the detector, j = 1 to 8.

- iv. Multiply the measured detector readings by the flux ratio T_{dj} to transform the measurements into the corresponding measured PMFD mesh fluxes. It should be noted that each detector reading gives 8 "measured" PMFD mesh fluxes.
- v. Use the "measured" PMFD mesh fluxes as internal boundary values to calculate the new flux/power distributions.

The above transformation procedure is not the only possible procedure. Other rigourous approaches based on transport theory can be implemented. However, the present procedure does have the following advantages:

- each transformation procedure takes less than two minutes on an Apollo-DN4500 microcomputer,
- ii. since a whole set of theoretically calculated detector readings is available, it is possible to reject erroneous measurements by comparing the actual measurements with the calculations, and

iii. the extra computational burden is insignificant because the transformation procedure needs to be performed infrequently, (a) after a refuelling operation, (b) after a significant change in reactivity device configuration, or (c) after a significant time has elapsed since the last transformation, e.g., more than one hour.

PMFD MODEL

The PMFD model is very similar to the model used in the conventional off-line fuel management program such as FMDP (Fuel Management Design Program). The present PMFD model for an uprated CANDU-6 SEU core includes 388 fuel channels and 152 reflector sites in the radial plane. There are twelve axial meshes. Each axial mesh, which is one fuel-bundle in length, has a unique set of lattice properties according to the type of fuel bundle and the current irradiation. The PMFD program can be initialized at any instance by downloading the appropriate fuel irradiation distribution from any off-line fuel management program. Starting from this point, PMFD will update the fuel burnup distribution in the core continuously according to the reactor power history and refuelling schedules. The power distribution in the core at any time can be calculated on demand, always using the most up to date information.

The simple PMFD model used in this study was developed on an IBM XT with only 640 K RAM. Modern microcomputers can easily accommodate a fine-mesh PMFD model with complexity comparable to the off-line FMDP model used in fuel management studies.

EXECUTION SPEED

PMFD has been implemented in many different computers, from the humble IBM PC to the modern CDC Cyber 990. Table 1 gives the execution speeds of PMFD on various machines. These machines, with the exception of the CDC machines, are relatively inexpensive microcomputers. However, some of these microcomputers are more powerful than the existing CANDU 6 control computer. It should be noted that PMFD can be executed in less than two minutes on an Apollo DN 4500 microcomputer equipped with a Weitek floating point accelerator. At this speed, PMFD can easily replace the Flux Mapping program for spatial control purpose.

It is also significant that the PMFD program can be executed in less than ten seconds on the CRNL CDC Cyber 990 computer. This suggests that reasonably fast power transients resulting from loss of regulation incident can be tracked using PMFD. Of course, fast response detectors such as inconel or platinum-plated inconel will have to be used for this purpose.

The speed of microcomputers such as the Apollo DN series computers have been increasing rapidly in the last few years. New microprocessors which are more than ten times faster than the DN4500 are now available. Furthermore, the new microcomputers are often designed to have several microprocessors operating in parallel. The new Apollo DN 10000 computer, for example, is designed to have up to 4 CPUs (Central Processing Units) operating in parallel. The speed of each CPU is approximately five times faster than the DN 4500. The price/performance ratio of all computers is expected to drop significantly in the next few years. Therefore, it is entirely feasible to design a PMFD program today to run on a future computer which has ten or more CPUs operating in parallel. Such a computer will be able to execute the PMFD program in less than one second. Thus, for all practical purposes, the speed of PMFD for on-line applications is not an issue.

PERFORMANCE OF PMFD

If flux detectors are not used as internal boundary conditions, PMFD will give the same results as FMDP, provided that the same mesh structure and the same lattice parameters are used in both programs. The accuracy of PMFD, without using measured flux detector readings, can be as good as any conventional off-line fuel management program simply by increasing the complexity of the PMFD model. Many fast microcomputers such as the Apollo DN10000, which can execute a detailed PMFD model in less than 2 minutes, are now available at affordable prices.

The advantage of using measured detector readings depends on how accurate the theoretical simulation model represents the real reactor. If the theoretical model is perfect, then using measured detector readings will not improve the accuracy of the simulation. The theoretical models, however, will not be perfect because there are always uncertainties in the reactivity device position measurements, the coolant densities, the fuel temperatures, the lattice parameters and the fuel burnup distribution used in the simulations. Because the detector readings are measured in the real reactor environment, incorporation of these measurement should improve the representation of the real reactor core in the simulation model and therefore should improve the simulation accuracy. This is the advantage of PMFD over conventional fuel management programs. The disadvantage is that PMFD accuracy will also be influenced by flux detector errors.

RANDOM DETECTOR ERRORS

The output from a Flux Mapping detector in an operating reactor consists of both true neutronic signal and random noise. The random noise comes from random neutronic fluctuations in the core and from the electronic hardware. The effect of the noise component at any particular detector at any particular time is a random phenomenon. It can either increase or decrease the output of a detector with respect to the true neutronic signal. The random error component of the detector signal is completely unpredictable and cannot be filtered out. However, the effect of random detector error on the power mapping accuracy of either Flux Mapping or PMFD can be simulated by multiplying the measured detector readings by a set of random error factors. These random error factors are generated by a computer program using a random number generator. Each set of random error factors consists of 102 numbers, corresponding to each of the 102 flux detectors used in the CANDU 6 reactors. The distribution of the random error factors in each set is a normalized Gaussian distribution with a specified standard deviation, typically 0.05 in Flux Mapping analyses. It is necessary to carry out the flux or power mapping procedure with several sets of random factors in order to evaluate the random error effect on a statistical basis.

The effect of random detector errors on PMFD mapping accuracy has been evaluated by using 10 sets of random detector error factors, which have a mean of 1.00 and a normalized standard deviation of 0.05. The results are given in Table 2. The average degradation in PMFD accuracy is about 1.0% rms for channel powers and 1.2% for bundle powers. Previous studies performed for Ontario Hydro reactors indicated that the corresponding degradation in Flux Mapping accuracy would be 1.3% rms for channel powers. The corresponding degradation for bundle powers are not available because Flux Mapping does not give full core bundle power distributions. PMFD is not sensitive to random detector error because the reactor flux and power shapes are mostly determined by the fuel burnup distribution and reactivity device configurations. The sensitivity of PMFD to random detector errors will be further reduced in a fine-mesh PMFD model because the influence of the measured detector readings will be reduced in a larger model.

SYSTEMATIC ERRORS

There are two major sources of systematic errors:

- i. some detectors are consistently giving higher or lower readings than the true flux levels, and
- ii. systematic loss of detector signals.

Because PMFD can be carried out independent of the flux detectors, it can be used to detect any systematic errors in (i), which are mainly due to incorrect calibration of the detectors. A set of theoretical detector readings can be produced by PMFD at any instance without using detector readings. These theoretical readings can be compared with the corresponding measurements. Several such comparisons over a reasonable time period will establish a pattern which will expose the systematic errors. These systematic errors can be eliminated by calibrating the suspected in-core flux detectors with a "Travelling Flux Detector", which has been specifically developed by AECL for this purpose.

The current Flux Mapping program in the natural CANDU 6 reactors depends exclusively on the flux detector readings to synthesize the reactor flux distribution from a precalculated set of harmonic flux modes. The locations of the flux detectors have been carefully chosen to match the spatial distribution of the harmonic flux shapes. The failure of a significant number of detectors, especially if they are concentrated in one location, e.g., in the same flux detector rod assembly, may artificially weaken the amplitudes of some crucial harmonic flux modes in the synthesized flux shape. This kind of systematic error could significantly affect the accuracy of the Flux Mapping program. The PMFD program, on the other hand, generates most of the information through the diffusion calculation, which depends mainly on the fuel irradiation and reactivity device configuration only. Whereas detector signals are crucial in Flux Mapping, they are merely enhancements in PMFD. Therefore, PMFD is not expected to be sensitive to the systematic loss of detector signals.

Two PMFD simulations have been carried out to assess the sensitivity of PMFD to the loss of all detector signals in:

- i. a corner flux detector assembly which has 4 detectors, and
- ii. a central flux detector assembly which also has 4 detectors.

The results of the above analysis are summarized in Table 3. As expected, the degradation in PMFD accuracy due to the systematic loss of detector signals is minimal, i.e., less than 0.1% rms in both cases.

LATTICE CROSS SECTION ERROR

The accuracy of any diffusion codes, such as FMDP and PMFD, depends on the accuracy of the lattice parameters, e.g., absorption and fission cross sections, used in the simulations. There are always uncertainties in these lattice parameters because the concentrations of the uranium and plutonium isotopes in each fuel bundle in the core cannot be calculated with absolute accuracy. The flux detectors, however, measure the exact state of the operating reactor, including all the details which cannot be represented in the theoretical model. The additional information provided by the detector readings should improve the accuracy of the diffusion calculation.

PMFD simulations have been carried out to assess:

- i. the sensitivity of PMFD to inaccuracies in input lattice cross sections, and
- ii. the improvements in the simulation accuracy by incorporating detector readings.

In these simulations, the reactor was operating in the shim mode with four corner adjuster rods raised out of the core. The reference reactor power shape was calculated with PMFD using distributed xenon properties corresponding to this power shape.

Another PMFD simulation was carried out using uniform xenon properties and without using flux detector readings. The maximum difference in the thermal absorption cross section between these two simulations is \pm 1%. The difference in the power distributions between these two PMFD simulations represents the error of the diffusion calculation due to an uncertainty of \pm 1% in the lattice cross sections.

A final PMFD simulation was carried out using uniform xenon properties and using flux detector readings extracted from the reference case. The results of the simulations are summarized in Table 4 and illustrated in Figures 3 and 4. It can be seen that the use of flux detector readings significantly reduces the power mapping error which arises from the uncertainties in the lattice cross sections used in the diffusion calculation.

ZONE CONTROLLER LEVEL INDICATION ERROR

The PMFD program was used to assess the error in diffusion calculations due to the uncertainty in zone controller level indications. The reference power shape was calculated by PMFD with the two top zone controllers in the central assemblies operating at 40% fill and the remaining zone controllers at 50% fill. It was assumed that because of indication error, all zone controllers were reported to be operating at 50% fill. A PMFD simulation was carried out with all zone controllers set at 50% fill and without using flux detector readings. The discrepancy between these two PMFD simulations represents the simulation errors due to errors in zone controller level indications. Another PMFD simulation was carried out with all the zone controllers set at 50% fill and also using flux detector readings extracted from the reference case.

The results of these simulations are summarized in Table 5 and illustrated in Figures 5 and 6. It is clear that using detector readings in PMFD substantially reduces the simulation errors due to inaccurate zone controller level indications.

COMPARISON OF PMFD AND FLUX MAPPING IN POINT LEPREAU

The superior performance of PMFD can be demonstrated using the data obtained from Flux Mapping measurement carried out in Point Lepreau in December 1984. A very accurate set of vanadium Flux Mapping detector readings was obtained at Point Lepreau with the reactor operating at 100% full power. The channel powers derived from Flux Mapping using the measured detector readings were compared with the FMDP simulation of the reactor at the time of measurement. Figure 7 shows the percentage error between Flux Mapping derived channel powers and FMDP channel powers. It can be seen that the rms channel power mapping error for the Flux Mapping program is 3.69%. It is also evident that Flux Mapping underestimates the high power channels in the central region. For example, Flux Mapping underestimates the maximum channel power at K-12 by 6%.

A corresponding channel power map was generated by PMFD using the same set of measured flux detector readings. It can be seen from Figure 8 that the rms channel power mapping error for PMFD is only 1.76%. The improvement in mapping accuracy is especially significant in the central high power region. For example, the discrepancy between FMDP and PMFD at the maximum power channel (K-12) is only 0.4%. It should be noted that the agreement between PMFD and FMDP can be further improved by adding more meshes to the PMFD model.

DESIGN CONCEPT OF PMFD MAPPING SYSTEM FOR THE REACTOR POWER CONTROL SYSTEM

The on-line PMFD based Power Mapping program (Figure 9) will have a role similar to that of the Flux Mapping program in CANDU 6. The technique that will be used for the calculation of various maps will be based on PMFD, rather than using linear modal expansion technique presently used in CANDU 6 Flux Mapping.

The Power Mapping program, similar to Flux Mapping program, should be executed at least at two minute intervals.

Vanadium detector signals will be read, checked for rationality, converted to flux and corrected for detector sensitivity. In the program, provision will be made for compensating for differences from detector to detector caused by:

- unavoidable small sensitivity differences built into the detectors during manufacturing,
- small sensitivity differences due to localized flux depression effects caused by other detectors at the same elevation, and
- sensitivity differences caused by detector burnup as the vanadium nuclei in the detector are converted to chromium as a result of the neutron-capture and beta decay process which produces the electrical signal.

An error detection algorithm will be provided for the detection of vanadium detector that are badly in error. Failed detectors of SIR type can be replaced on-line. However, in practice replacement may be deferred, until a convenient time. Thus, to minimize the degradation of PMFD mapping accuracy due to failed detectors or badly erroneous detectors, an on-line error detection feature and operator initiated detector rejection feature will be provided.

As part of the program input, the positions of the reactivity devices will be read and checked for rationality. Refuelled channels will be identified by the operator and read by the power mapping routine. The calibrated bulk power will be provided by the Power Measurement and Calibration routine of the Reactor Regulating System program.

The main outputs of the program, for spatial control purposes will be the fourteen Zone Powers. For neutronic setback the output of the program will be the value of High Bundle/Channel Power. All these are outputs to be sent to the Reactor Regulating System program.

Because of the dynamic characteristics of the vanadium flux detectors, the mapped Bundle/Channel powers will clearly not be suitable if the power is changing rapidly relative to the 5.4 minute time constant of the vanadium detectors. To overcome this shortcoming the mapped Bundle/Channel powers before being used by the setback routine will be adjusted on the basis of the fast measurement of bulk power. Also, because of the slow response of the vanadium detectors compared to the thermal power measurements, spatial calibration will not be allowed to interfere with bulk power regulation.

CONCLUSIONS

The PMFD approach has been found to be an accurate method of determining the zone-average power, which is the primary feedback variable used in CANDU spatial control, and in determining individual bundle and channel powers, which are equally important especially for neutronic setback. As for the computational speed, computers are readily available today, at moderate prices to solve a detailed PMFD model on-line within two minutes. Also, PMFD has been found to have low sensitivity to various errors. A comparison with Flux Mapping data obtained from Point Lepreau indicates that the PMFD accuracy is superior.

REFERENCES

- E. Hinchley and G. Kugler, "On-Line Control of CANDU-PHW Power Distribution", AECL-5045, March 1975.
- P.S.W. Chan and A.R. Dastur, "The Role of Enriched Fuel in CANDU Power Uprating", Proceedings of the 8th Annual Conference, Canadian Nuclear Society, Saint John, New Brunswick, June 1987.
- 3. P.F. Zweifel, "Reactor Physics", McGraw-Hill Book Company, 1973.
- 4. Roger A. Ryden, "Nuclear Reactor Theory and Design", University Publications, 1977.

TABLE 1

PMFD EXECUTION SPEED ON VARIOUS MACHINES

MACHINE	MAIN PROCESSOR	MATH COPROCESSOR	TIME FOR* 1 FLUX ITERATION (sec)	RELATIVE CPU SPEED	PMFD EXECUTION TIME (sec)
XT Clone	8 MHz-8088	8 MHz-8087	27.1	1.0	2710
AT Clone	12 MHz-80286	10 MHz-80287	13.4	2.0	1340
Toshiba T5100 Lap Top	16 MHz-80386	16 MHz-80387	5.7	4.8	570
AST-20 Desk Top	20 MHz-80386	20 MHz-80387	4.3	6.3	430
Apollo DN 3010	16 MHz-68020	16 MHz-68881	10.1	2.7	1010
Apollo DN 4500	33 MHz-68030	33 MHz-68882	3.1	8.7	310
Apollo+ DN 4500	33 MHz-68030	Weitek FPA	1.0	27.1	100
Apollo DN 10000	PRISM-RISC	_	0.20	135.5	20
CDC Cyber 830		-	2.0	13.6	200
CDC Cyber 990	(low optimization)	_	0.16	169.4	16
CDC Cyber 990	(high optimization)	_	0.09	301.1	9

^{* 540} x 12 mesh points, 2 neutron energy groups.

⁺ 0.5 -> 1.0 MFLOP (millions of floating point operations per second).

TABLE 2
EFFECT OF RANDOM DETECTOR ERRORS ON PMFD ACCURACY

RANDOM ERROR PATTERN *	RMS MAPPING ERROR		
	CHANNEL POWER	BUNDLE POWER	
1	0.74	1.02	
2	1.05	1.38	
3	0.82	1.30	
4	1.42	1.31	
5	1.12	1.18	
6	1.10	0.91	
. 7	1.11	0.99	
8	0.80	1.65	
9	1.14	1.21	
10	1.11	0.73	
AVERAGE	1.04	1.17	

^{*} σ for random error = 0.05

TABLE 3
EFFECT OF LOSS OF DETECTOR SIGNALS ON PMFD ACCURACY

FAILED DETECTOR ASSEMBLY	RMS MAPPING ERROR	
	CHANNEL POWER	BUNDLE POWER
VFD1 *	0.07	0.09
VFD14 **	0.05	0.08

^{*} VFD1 is a corner assembly with 4 flux detectors

^{**} VFD14 is a central assembly with 4 flux detectors

TABLE 4

EFFECT OF LATTICE CROSS SECTION ERROR *
ON PMFD ACCURACY

	ERROR (%)	
	WITHOUT DETECTOR	WITH DETECTORS
Maximum Channel Power	0.30	0.07
Maximum Bundle Power	3.23	0.40
rms error Channel Power	1.77	0.62
rms error Bundle Power	2.81	0.87
Zone 1	-0.06	0.10
Zone 2	0.93	0.02
Zone 3	1.90	0.07
Zone 4	1.31	0.02
Zone 5	-0.33	-0.05
Zone 6	0.68	-0.04
Zone 7	1.41	-0.10
Zone 8	- 1.08	0.11
Zone 9	0.43	0.03
Zone 10	-3.02	0.07
Zone 11	0.60	-0.01
Cone 12	-0.50	-0.06
Zone 13	0.51	-0.04
Zone 14	2.05	-0.10

^{* ±1%} error in thermal absorption cross section

TABLE 5

EFFECT OF ZONE CONTROLLER LEVEL ERROR ON PMFD ACCURACY

	ERROR (%)	
	WITHOUT DETECTOR	WITH DETECTORS
Maximum Channel Power	- 0.30	-0.15
Maximum Bundle Power	- 2.21	-1.01
rms error Channel Power	1.32	0.38
rms error Bundle Power	1.35	0.46
Zone 1	0.94	0.13
Zone 2	-0.11	0.39
Zone 3	- 0.98	-0.12
Zone 4	0.30	0.18
Zone 5 *	- 2.48	-0.26
Zone 6	0.79	-0.12
Zone 7	- 0.29	0.12
Zone 8	0.98	0.01
Zone 9	0.07	0.34
Zone 10	0.98	-0.22
Zone 11	0.41	0.04
Zone 12 *	- 2.01	-0.28
Zone 13	0.80	-0.19
Zone 14	- 0.15	0.05

^{*} Zone levels in zone controllers 5 and 12 were increased from 40% to 50% fill to simulate zone level indication error

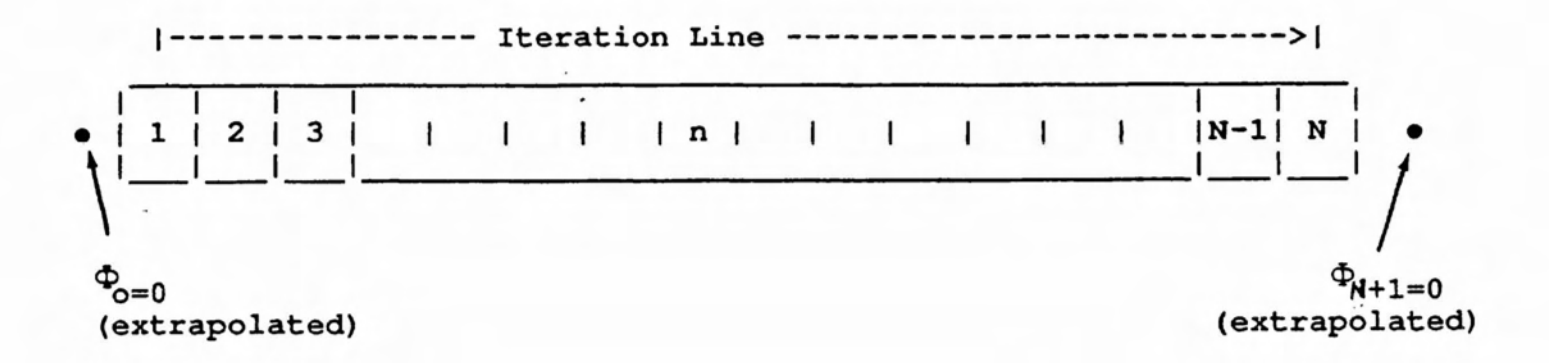


FIGURE 1 AXIAL MESHES IN A CHANNEL WITH EXTERNAL BOUNDARY CONDITIONS ONLY

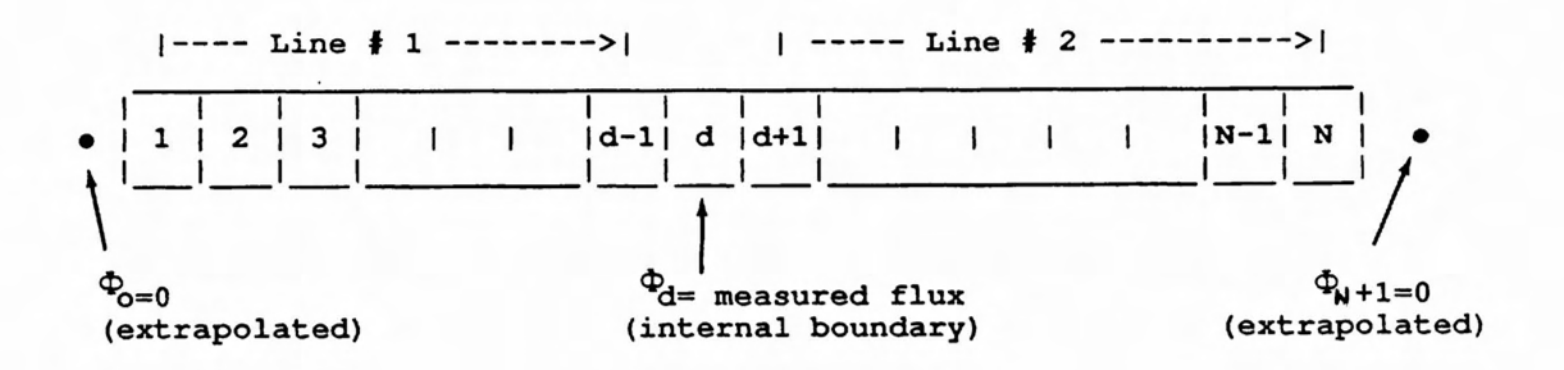
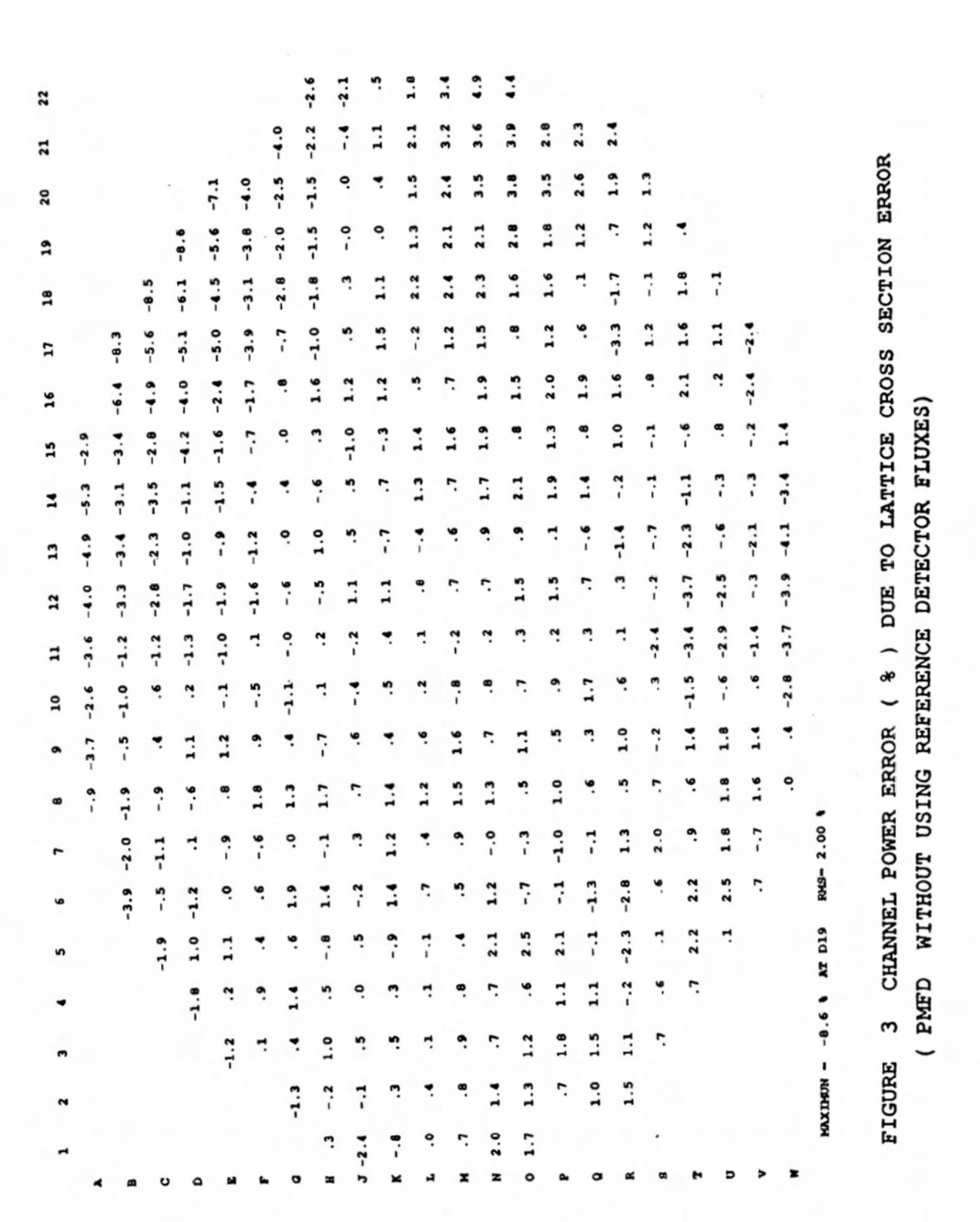
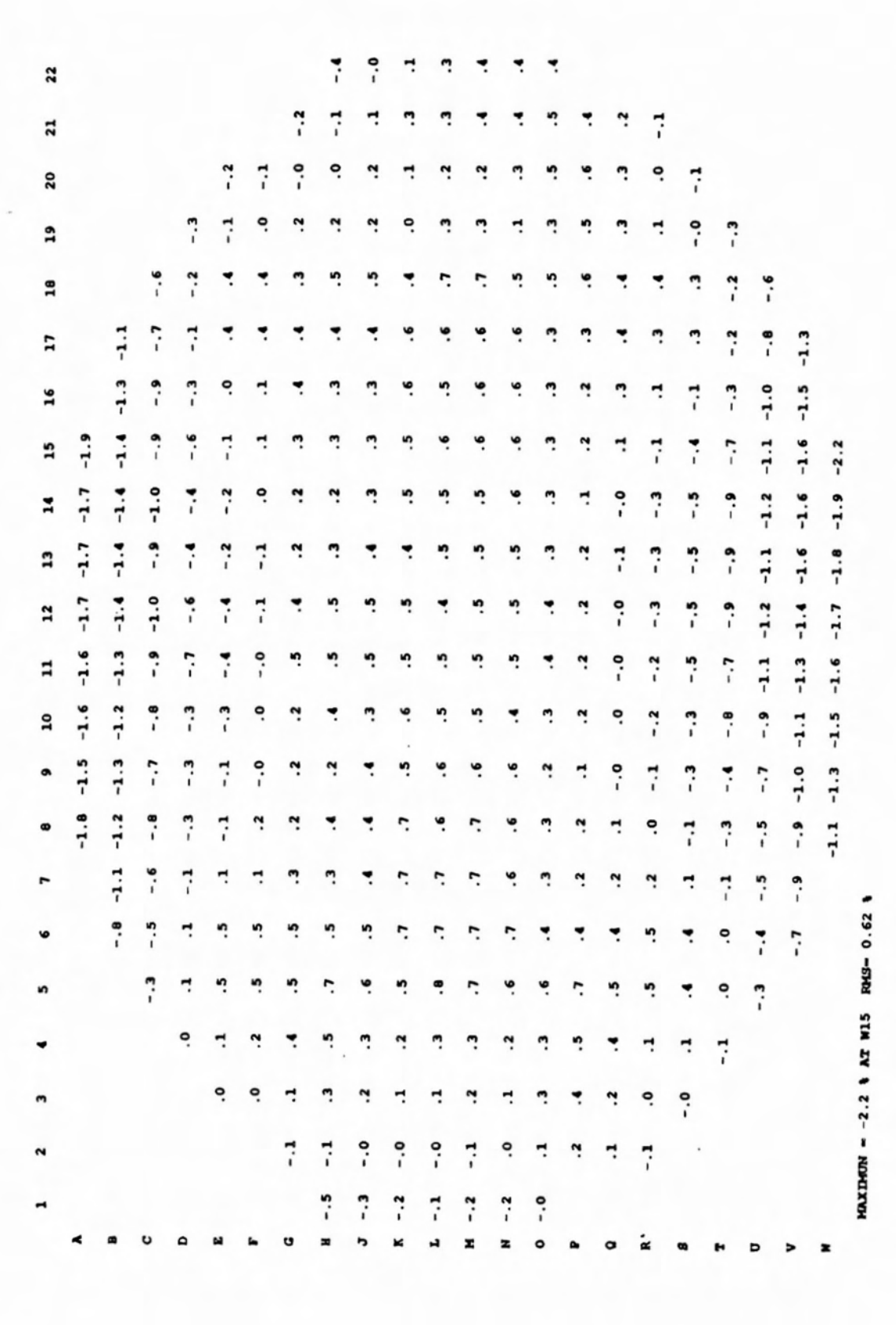
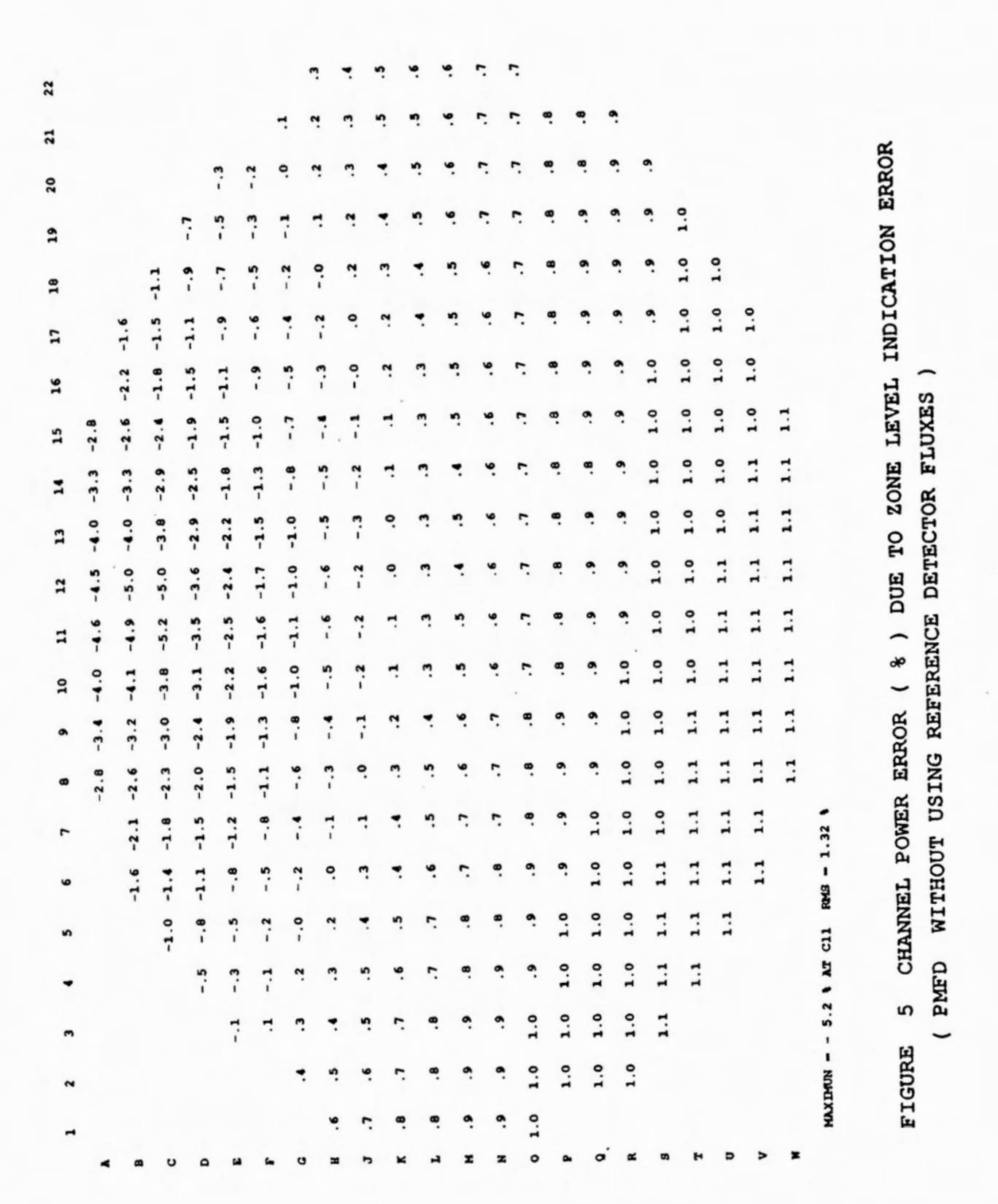


FIGURE 2 AXIAL MESHES IN A CHANNEL WITH EXTERNAL BOUNDARY
CONDITIONS AND MEASURED FLUX AS INTERNAL BOUNDARY VALUE





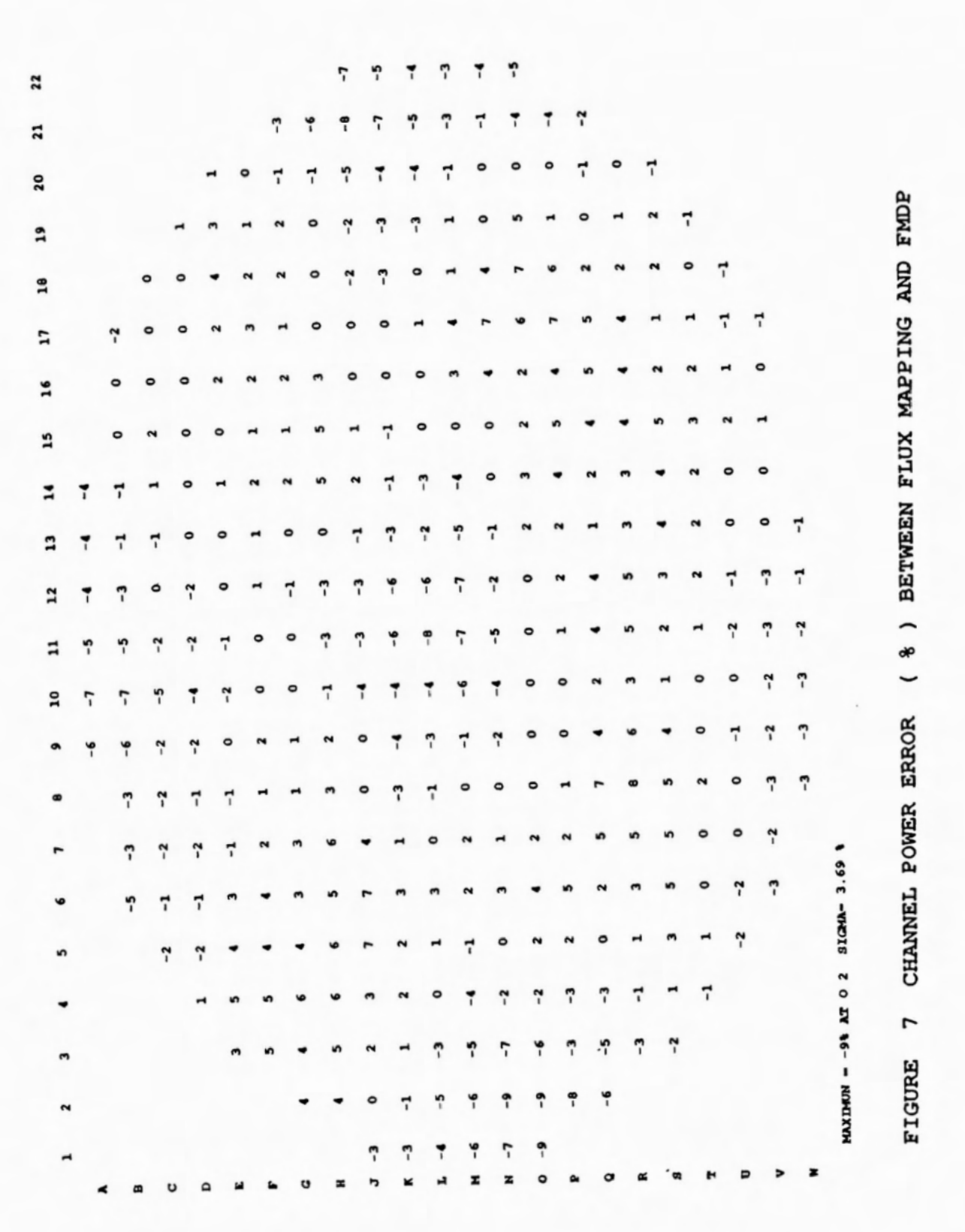
CHANNEL POWER ERROR (%) DUE TO LATTICE CROSS SECTION ERROR DETECTOR FLUXES USING REFERENCE PMFD FIGURE



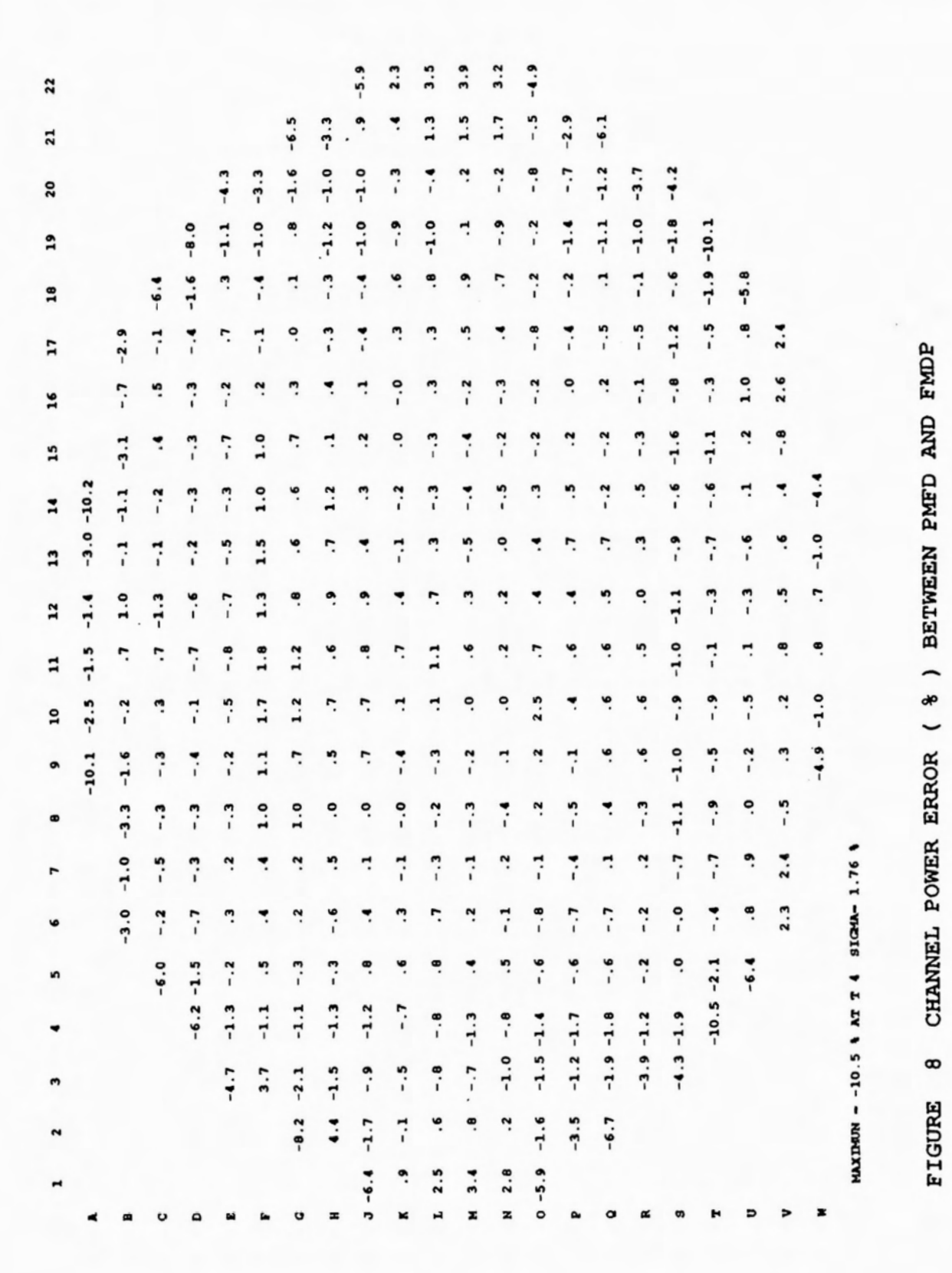
. 3 . 3 . 3 .1 . 3 . 2 .1 .1

MAXIMUN - -2.1% AT B12 RMS- 0.38 %

FIGURE 6 CHANNEL POWER ERROR (%) DUE TO ZONE LEVEL INDICATION ERROR (PMFD USING REFERENCE DETECTOR FLUXES)



- 277 -



- 278 -

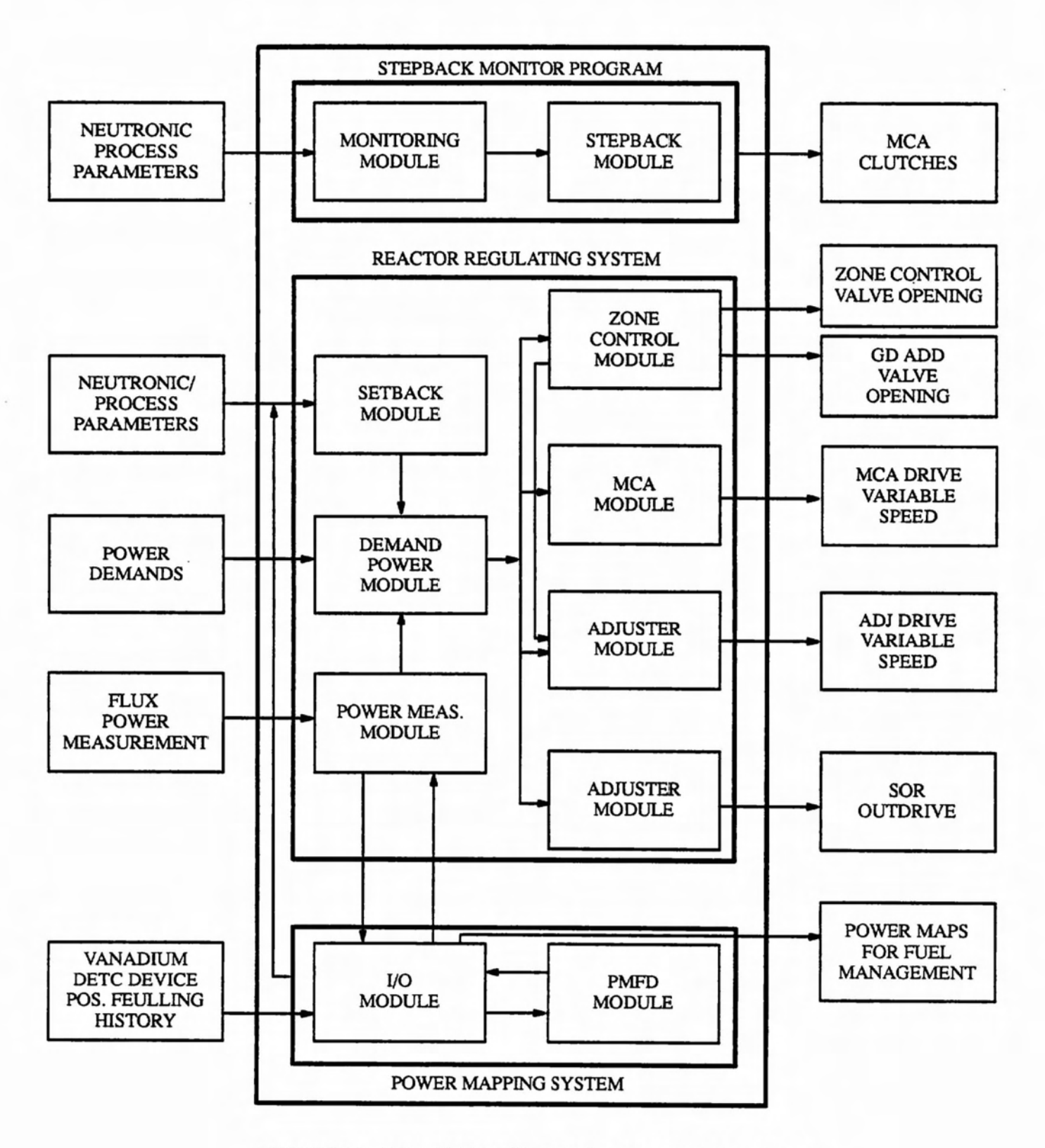


FIGURE 9: REACTOR CONTROL BLOCK DIAGRAM